DISCLAIMER NOTICE

THIS DOCUMENT IS BEST QUALITY PRACTICABLE. THE COPY FURNISHED TO DTIC CONTAINED A SIGNIFICANT NUMBER OF PAGES WHICH DO NOT REPRODUCE LEGIBLY.

COLD WORK AND THE DUCTILE-BRITTLE TRANSITION OF SILVER CHLORIDE

Twentieth Technical Report

By

T. S. Liu

R. J. Stokes

C. H. Li

Office of Naval Research Project

Nonr-4076(00) NR-032-451

June 1963

HONEYWELL

HR-63-266

COLD WORK AND THE DUCTILE-BRITTLE TRANSITION OF SILVER CHLORIDE

Twentieth Technical Report

by

T. S. Liu

R. J. Stokes

C. H. Li

Office of Naval Research Project

Nonr-4076(00) NR-032-451

June 1963

Honeywell Research Center

Hopkins, Minnesota

ABSTRACT

Polycrystalline silver chloride specimens having different microstructures were prepared by extruding monocrystals or precompressed powder at varying temperatures. Extrusion at high temperature (370°C) produced a fully recrystallized equiaxed material which was brittle and fractured by simple cleavage below its transition temperature (60°C for notched specimens). Extrusion at low temperatures (down to -196°C) produced an extremely tough cold worked material with grains elongated in the extrusion direction. This material fractured below its transition temperature (which varied from -20°C to -200°C) by an intergranular mode.

It is concluded that cold work increases the resistance to transgranular cleavage. Fracture is then deflected to propagate intergranularly over surfaces making an angle with the tensile axis with a corresponding improvement in notch toughness. This deflection is greater for extruded powder than for extruded monocrystals because of the extremely elongated grain shape.

TABLE OF CONTENTS

LIST OF ILLUSTRATIONS

LIST OF ILLUSTRATIONS (Cont.)

I. INTRODUCTION

Previous work[1], [2] on the fracture properties of fully recrystallized silver chloride under notch impact conditions has indicated that the fracture behavior is rather invariant. Thus polycrystalline materials originating from a number of sources ranging from relatively pure Harshaw single crystals to commercial purity powder and prepared by hot extrusion at 370°C, all fracture by simple cleavage with ductile brittle transition at 60°C (see Fig. 1). This behavior is also typical for fully annealed single crystals and appears to be fundamental to silver chloride for the particular loading conditions and notch configuration adopted.

One way in which this characteristic fracture behavior can be modified is by the dispersion of alumina particles in the silver chloride matrix[2]. Then, particularly when the alumina particles are in the shape of spheres, the ductive brittle transition is much less sharply defined and occurs over a range of temperature, the transition temperature is lowered considerably and the fracture mode changes from simple cleavage to a fibrous or shear mode. The reason for this change is believed to be partly due to the nucleation of cavities in the region of the dispersed alumina particles which influences the state of stress locally and the distribution of plastic constraint at the root of the notch. It is emphasized however that this is not the sole factor responsible for the increase in toughness. In extruded materials it is reasonable to expect that the resultant grain size, texture, and the residual cold work will be influenced by the presence of a dispersed phase.

The importance of cold work in crack propagation was discussed to a certain extent by Friedel[3] who analyzed the relationship between the propagation of cracks and the work hardening characteristics of semi brittle solids. He discussed the various ways in which plastic deformation could inhibit cleavage

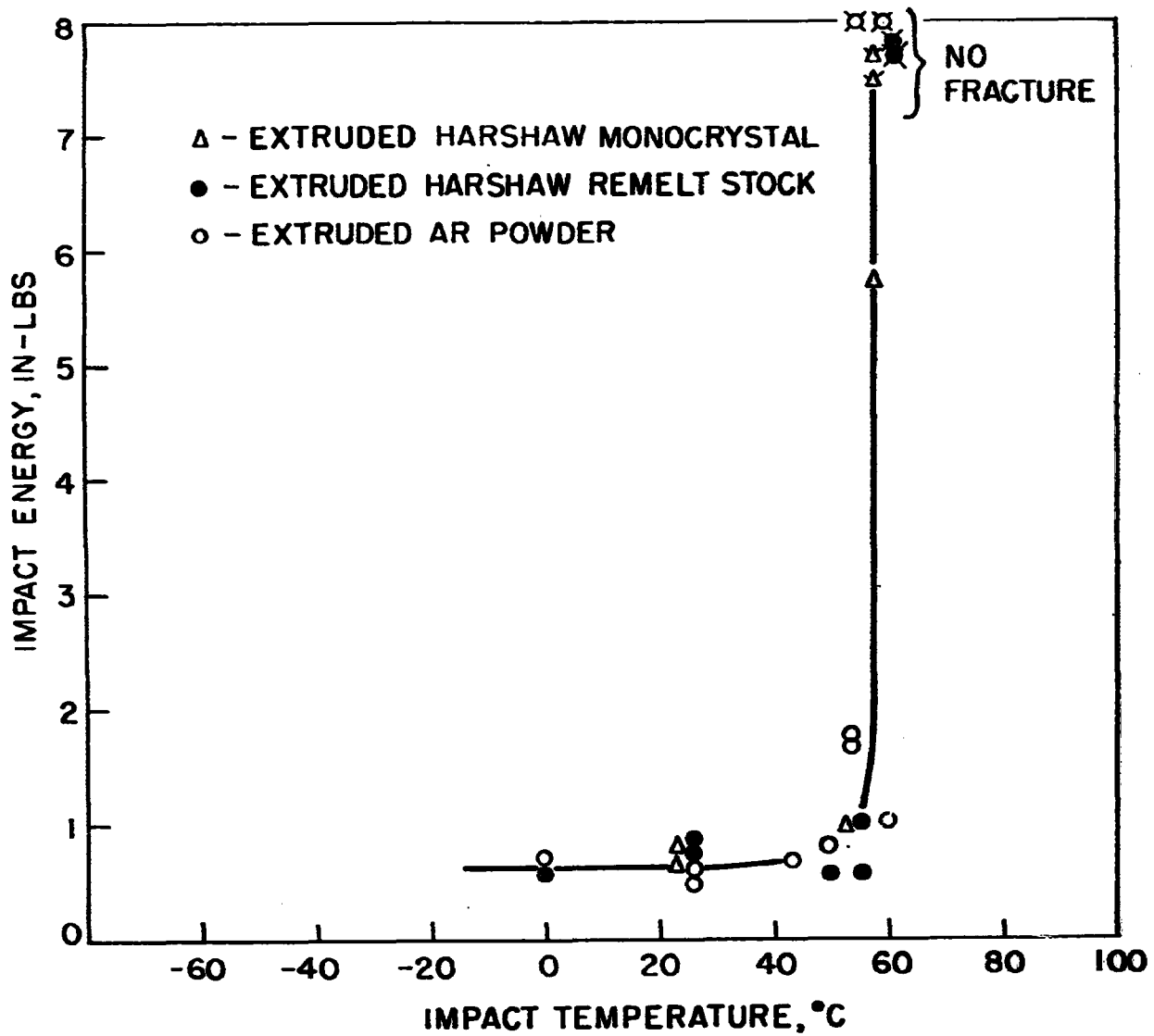

Figure 1 - Ductile-Brittle Transition Curves of Silver Chloride Polycrystals. Prepared by 370° C Extrusions

fracture propagation. Briefly, blunting by local slip at the crack tips, the interaction of cracks with dislocations introduced by prior cold work and plastic relaxation accompanying crack propagation all contribute to the resistance to crack propagation.

The present experiments were designed to determine the extent to which cold work influenced the fundamental ductile brittle transition temperature and fracture mode of silver chloride. They were stimulated by the discovery that silver chloride could be extruded at temperatures as low as -25°C when commercial purity powder was used and as low as -196°C when single crystals were used. This working temperature was far below that previously used (370°C) and it was found very early that such extruded material was exceedingly tough. The reasons for the enhanced toughness and its relation to the previous work on silver chloride-alumina compacts will be discussed.

II. EXPERIMENTAL PROCEDURE

A. MATERIALS USED

Two forms of silver chloride were used in this study; (1) silver chloride powder of analytical reagent (AR) grade with an average particle size of 6μ obtained from the Mallinckrodt Chemical Works (St. Louis, Missouri); (ii) optically pure monocrystals of silver chloride purchased from the Harshaw Chemical Company (Cleveland, Ohio).

B. PREPARATION OF THE EXTRUSIONS

The extrusion technique used for this investigation was similar to that described previously[2] in which a cold pressed billet or a cylindrical single crystal was extruded with a 16:1 reduction through a steel die to produce a rod of 3/16" diameter. The major difference was that a range of extrusion temperatures was employed. When AR powder was used as starting material, sound extrusions with a good smooth surface could be obtained at extrusion temperatures as low as -25°C. With monocrystals as starting material it was possible to obtain sound extrusions at even lower temperatures, down to -196°C.

C. IMPACT TESTS

The ductile-brittle transition and the fracture behavior of extruded silver chloride monocrystals and powder were investigated by subjecting specimens to impact bending tests at various temperatures. The impact specimens were supported, 1-1/16" apart, at each end and subjected to an impact loading at mid-span with a swinging pendulum. At the moment of impact, the strain rate at the outermost fiber of an unnotched specimen was 60 per second.

The preparation of unnotched impact specimens was as reported previously, rods 1-1/4" in length were cut from the extrusion and chemically polished before testing. The notched specimens were prepared by rolling or by machining (in those instances where rolling caused the specimens to crack) flat parallel surfaces and then cutting a 90° notch 0.025" deep with a razor blade.

The following baths were used to heat or cool the specimens prior to impact testing. Temperatures between 20°C and 175°C were obtained with a heated bath of mineral oil. For sub-zero temperatures iso-pentane cooled by liquid nitrogen was used and liquid nitrogen and liquid oxygen were used at their boiling points. Below liquid nitrogen temperature specimens were lowered inside a liquid helium container to a point above the liquid level corresponding to the desired temperature. In all cases at least five minutes were allowed for the specimens to come to thermal equilibrium and it was estimated that at the moment of impact the specimens were within ± 3°C of the intended temperature for temperatures down to liquid nitrogen and within +10°C for temperatures below liquid nitrogen temperature.

D. COMPRESSION TESTS

For the purpose of this investigation, it was not considered necessary to measure the absolute stored energy due to cold work by, for example, a calorimetric method. Instead,a semi-quantitative measurement of the relative amount of residual cold work was sought and to this end the simple yield stress under compression was used.

Specimens 0.080" x 0.080" cross section and .160" long were sectioned from the extrusions. These dimensions were chosen because they allowed at least three specimens to be prepared from approximate the same location along a given extrusion. Compression tests were performed in the Instron machine at a strain rate of 0.2×10^{-3} sec^{-1} at the beginning of the test. Lubricants were used to minimize friction at the end faces. All compression tests were performed at room temperature.

III. MICROSTRUCTURE OF LOW TEMPERATURE EXTRUSIONS

Regardless of the original source, whether monocrystalline or powder, the resultant extrusions were polycrystalline and fine grained with very elongated grains along the extrusion axes. Figure 2 depicts a typical transverse section and Figure 3 a typical longitudinal section (parallel to the extrusion direction) of an extracted single crystal. The grains in the cold worked regions were so fine that they could not be resolved at this magnification, the large grains were due to partial recrystallization which had also taken place. In a few instances full recrystallization occurred and the resulting fairly uniform equiaxed grains gave a microstructure similar to that produced by high temperature (370°C) extrusion as illustrated in Figure 4.

The partial recrystallization observed metallographically on extruded single crystals was also evident in their x-ray back reflection diffraction patterns shown in Figure 5. Due to the inhomogeneous nature of the grains in the majority of the specimens and the relatively small size of the x-ray beam (0.030") as compared with the specimen diameter (0.192"), a scanning technique was employed to obtain representative back-reflection patterns. In this technique, the polished longitudinal section of the specimen was exposed to the x-ray beam and scanned across its diameter repeatedly while its extrusion axis remained vertical and perpendicular to the x-ray beam. It can be observed that there is a certain degree of preferred orientation in the low temperature partially recrystallized extrusion of Figure 5. Comparison of the patterns from various extruded monocrystals worked at different low temperatures revealed that the same type and degree of preferred orientation persisted whenever recrystallization was incomplete. When full recrystallization occurred at high temperatures the back reflection pattern was as reproduced in Figure 6.

The grains resulting from the low temperature extrusion of AR silver chloride powder were too small and distorted to permit etching and convenient metallographic examination. Figure 7 is a scanning back reflection pattern taken on a powder specimen extruded at room temperature. Comparison with Figure 5 indicates the overall fineness of the grains and the lack of any large recrystallized grains. It will be noted also that there is a moderate preferred orientation with a texture different from that observed on extruded monocrystals. Again, comparison of the patterns obtained on AR powder extruded at different low temperatures revealed that the same degree and type of preferred orientation shown in Figure 7 persisted. When full recrystallization occurred during extrusion at high temperatures, the pattern was similar to Figure 6.

Figure 2 - Transverse Section of Extrusion Prepared from Monocrystal. Extruded at -150° C. X 200

Figure 2 - Transverse Section of Extrusion Prepared from Monocrystal. Extruded at -150° C. X 200

Figure 3 - Longitudinal Section of Extrusion Prepared from Monocrystal. Extruded at 50° C. X 200

Figure 3 - Longitudinal Section of Extrusion Prepared from Monocrystal. Extruded at 50° C. X 200

Figure 4 - Transverse Section of Extrusion Prepared from Monocrystal. Extruded at 370° C. X 200

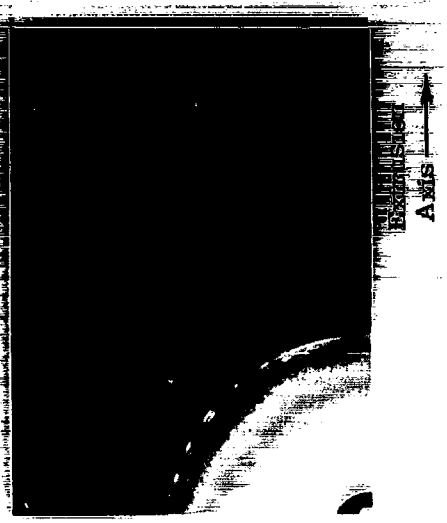

Figure 5 - Scanning Back Reflection Pattern of an Extrusion from Monocrystal. Extruded at 50° C.

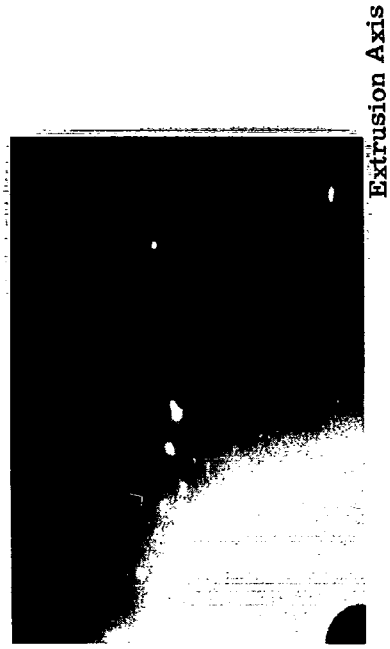

Figure 6 - Scanning Back Reflection Pattern of an Extrusion Prepared From Monocrystal. Extruded at 370° C.

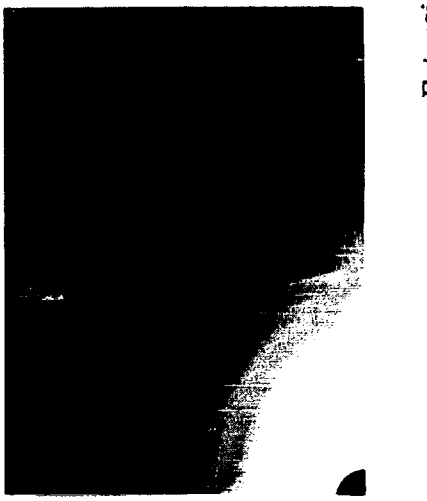

Figure 7 - Scanning Back Reflection Pattern of an Extrusion from AR Powder. (Extrusion temperature: room temperature).

IV. EXPERIMENTAL RESULTS

A. IMPACT ENERGY VS TEMPERATURE CURVES

Figures 8 and 9 summarize the impact energy-tempeature relationship for chemically polished, unnotched specimens prepared from extruded monocrystals and extruded AR silver chloride powder respectively. Figures 10 and 11 summarize the results for notched specimens prepared from extruded monocrystals and extruded powder respectively. It should be noted that for an energy absorption greater than 8 in-lbs. the specimens merely bent without fracturing.

The most remarkable observation was that in all instances where extrusion resulted in incomplete recrystallization, the nil-ductility temperature (the temperature at which the energy absorbed during impact began to increase) was lowered significantly. Thus, in the temperature range where completely recrystallized silver chloride is brittle and absorbs little energy in fracture, the extruded partially recrystallized material is much tougher and absorbs a higher amount of energy. On the whole, extruded powder is tougher than the equivalent extruded single crystal, as may be seen particularly by comparing Figures 10 and 11. An unnotched specimen of powder extruded at room temperature shows the ductile brittle transition below -220°C, the limit of the present testing procedure. The greatest effects of low temperature extrusion on the ductile brittle transition are to be found in the unnotched extruded monocrystals (Figure 8) where the transition temperature drops 150°C, and in notched extruded silver chloride power (Figure 11) where the transition temperature in some cases drops more then 200°C. (Note this 200°K drop is produced in a material that melts at only 700°K). Finally, it should be noted that some of the extrusions in Figure 11 show the ductile brittle transition over a wide range of temperatures whereas the phenomenon is much more sharply defined in the fully recrystallized material.

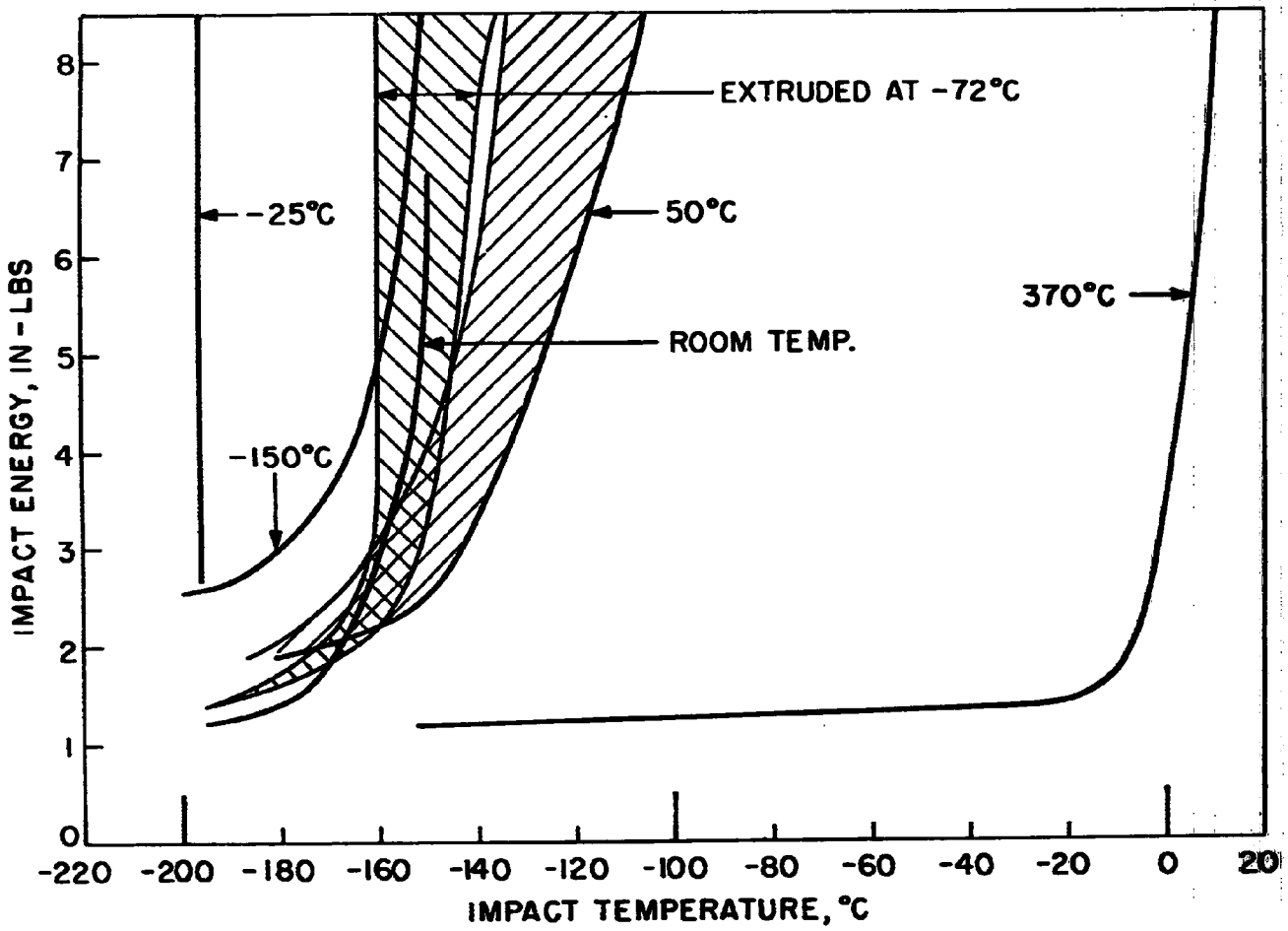

Figure 8 - Impact Transition for Extrusions from Monocrystals, Unnotched

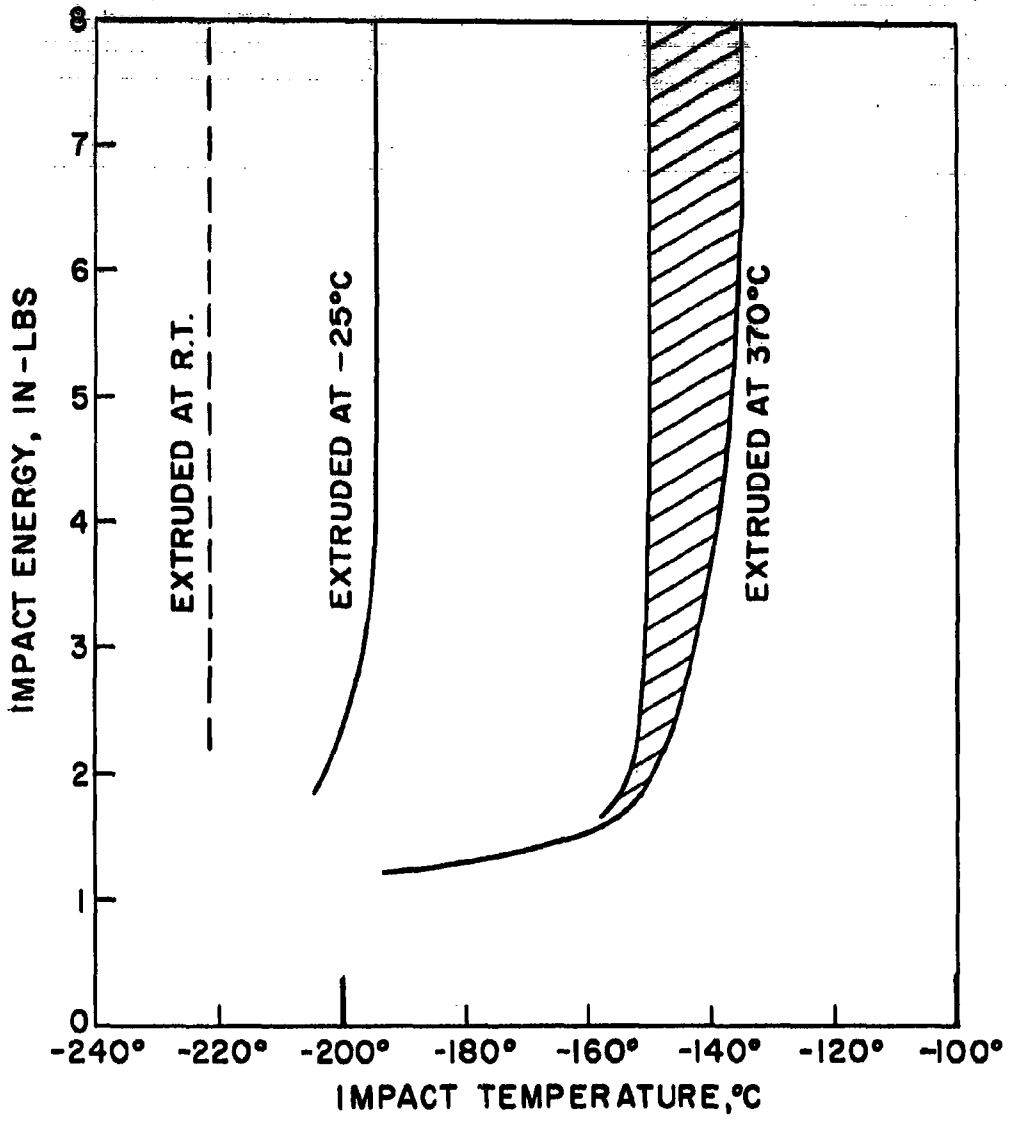

Figure 9 - Impact Transition for Extrusions from AR Powder, Unnotched

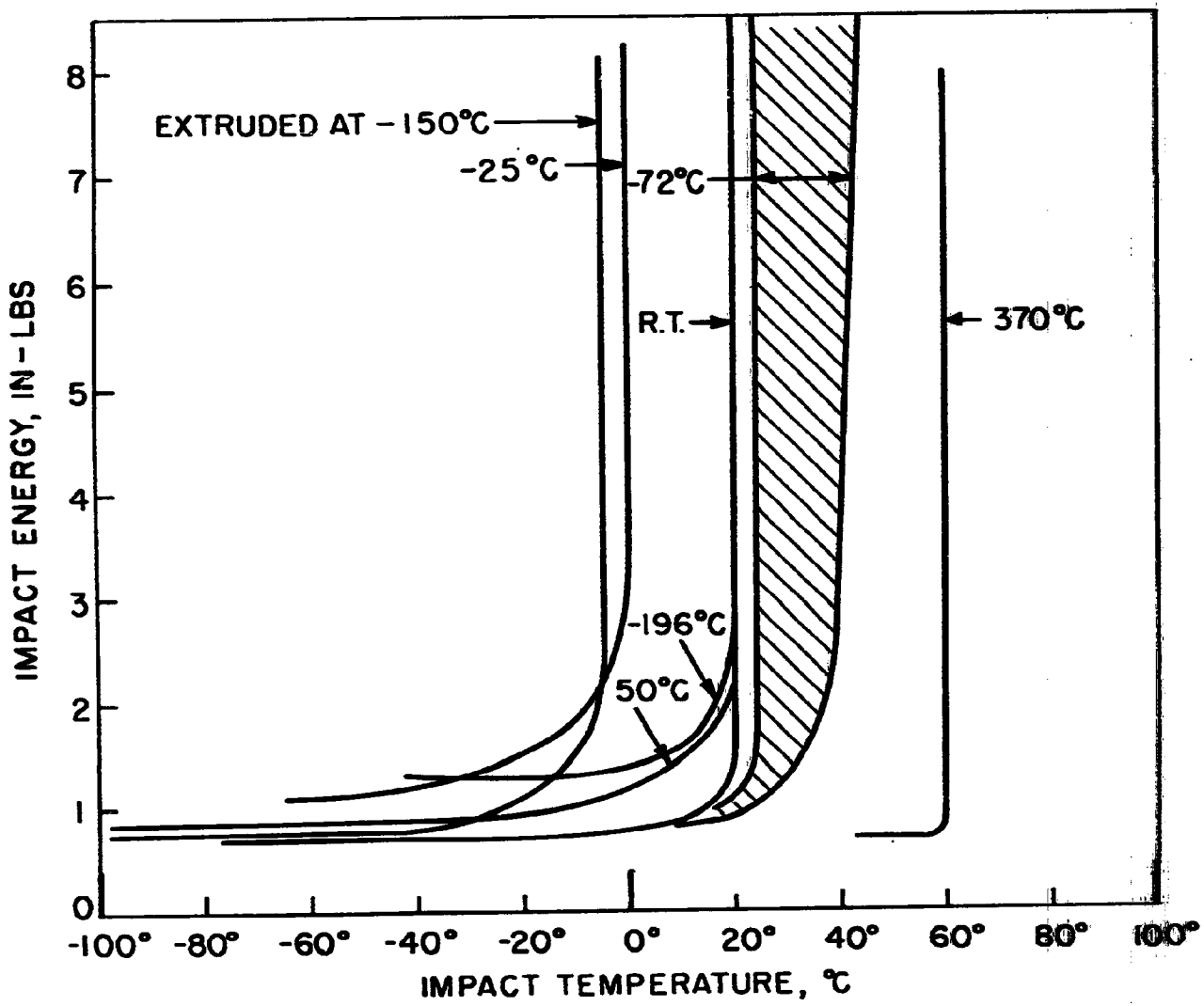

Figure 10 - Impact Transition for Extrusions from Monocrystals, Notched

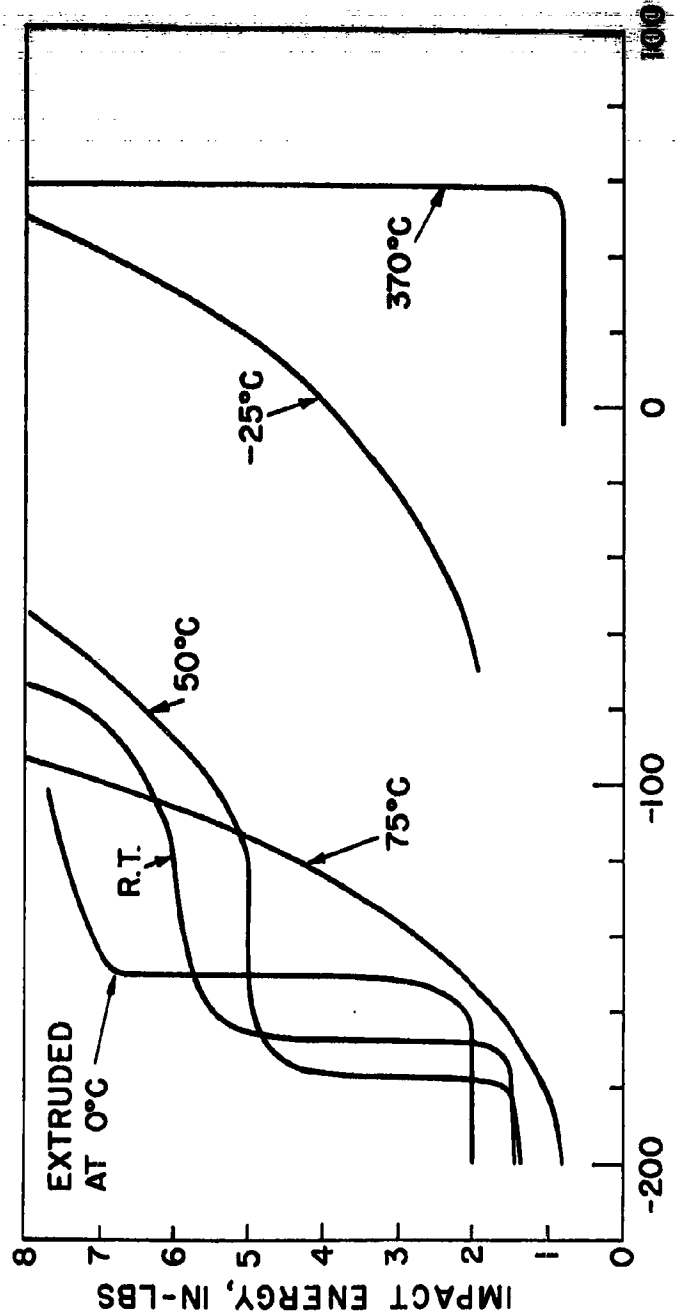

Figure 11 - Impact Transition for Extrusions from AR Powder, Notched.

B. FRACTURE SURFACE APPEARANCE

Fracture surfaces were examined with both the optical and electron microscopes. The technique for producing faithful replicas of the fracture surface for examination in the electron microscope has been described elsewhere[2].

1. Extruded Powder Compacts

It is convenient to describe the fracture surface appearance of extruded silver chloride powder compacts first. Figure 12 illustrates the macroscopic differences in fracture path for various notched specimens (the corresponding transition curves are in Figure 11). Fully recrystallized specimens (extruded at 370°C) fractured by simple cleavage, the fracture path was flat and normal to the tensile axis, as shown in Figure 12(a). As reported elsewhere[2] for silver chloride compacts containing 2-1/2 percent alumina spheres (also extruded at 370°C) the locus of the fracture surface was diverted and followed a zig-zag path approximately at 45° to the tensile axis or parallel to the surfaces of maximum shear stress, this is shown for comparison in Figure 12(b). For the low temperature powder extrusions the fracture path was strikingly different, as shown in Figure 12(c) and followed a surface considerably inclined to the tensile axis. The specimen shown in Figure 12(c) was extruded at room temperature and fractured in impact at liquid nitrogen temperature.

Figure 13 compares the macroscopic appearance of the fracture surface for fully recrystallized material (Figure 13(a)) and powder material extruded at low temperatures (Figure 13(b)). These should be related with Figures 12(a) and 12(c) respectively. The fully recrystallized material showed a typical specular cleavage surface with the origin of cleavage fracture located a short distance below the line of the notch. By contrast, the cold worked material had a rough satin macroscopic appearance typical of a shear fracture, with the origin located along the line of the notch.

B. FRACTURE SURFACE APPEARANCE

Fracture surfaces were examined with both the optical and electron microscopes. The technique for producing faithful replicas of the fracture surface for examination in the electron microscope has been described elsewhere[2].

1. Extruded Powder Compacts

It is convenient to describe the fracture surface appearance of extruded silver chloride powder compacts first. Figure 12 illustrates the macroscopic differences in fracture path for various notched specimens (the corresponding transition curves are in Figure 11). Fully recrystallized specimens (extruded at 370°C) fractured by simple cleavage, the fracture path was flat and normal to the tensile axis, as shown in Figure 12(a). As reported elsewhere[2] for silver chloride compacts containing 2-1/2 percent alumina spheres (also extruded at 370°C) the locus of the fracture surface was diverted and followed a zig-zag path approximately at 45° to the tensile axis or parallel to the surfaces of maximum shear stress, this is shown for comparison in Figure 12(b). For the low temperature powder extrusions the fracture path was strikingly different,as shown in Figure 12(c) and followed a surface considerably inclined to the tensile axis. The specimen shown in Figure 12(c) was extruded at room temperature and fractured in impact at liquid nitrogen temperature.

Figure 13 compares the macroscopic appearance of the fracture surface for fully recrystallized material (Figure 13(a)) and powder material extruded at low temperatures (Figure 13(b)). These should be related with Figures 12(a) and 12(c) respectively. The fully recrystallized material showed a typical specular cleavage surface with the origin of cleavage fracture located a short distance below the line of the notch. By contrast, the cold worked material had a rough satin macroscopic appearance typical of a shear fracture, with the origin located along the line of the notch.

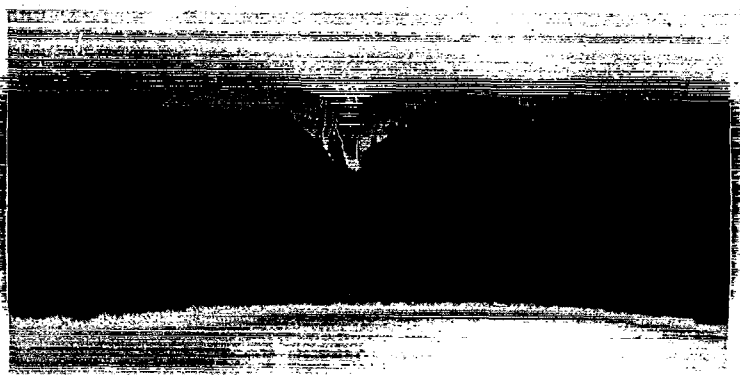

(a) AR Powder Extruded at 370° C. X 6

(b) AR Powder with 2-1/2 percent spherical alumina dispersion extruded at 370° C. X 6

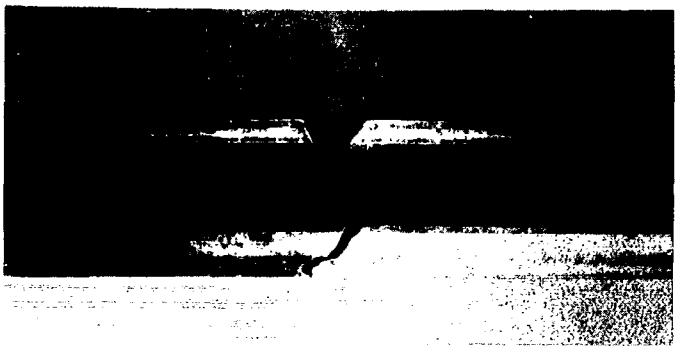

(c) AR Powder extruded at room temperature. X 10

Figure 12 - Macroscopic View of Various Fracture Plane Loci.

Figure 13(a) - Macroscopic View of Fracture Surface Observed on Extrusion from Monocrystals Extruded at 370° C. X 10

Figure 13(b) - Macroscopic View of Fracture of an Extrusion Made from AR Powder. Extruded at Room Temperature. X 8

Figure 13(a) - Macroscopic View of Fracture Surface Observed on Extrusion from Monocrystals Extruded at 370° C. X 10

Figure 13(b) - Macroscopic View of Fracture of an Extrusion Made from AR Powder. Extruded at Room Temperature. X 8

At higher optical magnification it could be seen that the origin of cleavage fracture in the fully recrystallized material in Figure 13(a) was intergranular, in agreement with previous observations[2]. Under the electron microscope the fracture surfaces presented a clear cut example of simple cleavage propatation as reproduced in Figure 14(a). But again the appearance of the fracture surface of the cold worked material under the electron microscope was strikingly different and is reproduced in Figure 14(b). There were no cleavage markings, nor were there any tear markings characteristic of a fibrous or shear type fracture as described in the previous paper[2], instead the grains and grain boundaries were distinct and at this magnification the features of intergranular fracture were unmistakable. The fine grain size and elongated appearance of the grains were consistent with the microstructure determined from the x-ray Laue back reflection pictures of Figure 7, the direction of elongation was found to be parallel with the extrusion axis.

The fracture surface appearance of unnotched specimens from powder extrusions showed essentially the same features as those reported here on the notched specimens.

On the basis of these observations it was deduced that in the heavily cold worked unrecrystallized polycrystalline material, the individual crystallites were severely distorted and elongated and the grain boundaries extremely jagged. This microstructure bore no resemblance to the ideal equiaxed grain boundary network in fully recrystallized material. It is important to point out that the full realization of this microstructure and an appreciation of the fracture mode was possible only with the utilization of the high resolution electron fractographic technique, optically the surface had the appearance of a shear fracture.

Figure 14(a) - Electron Micrograph of Fracture of Extrusions Made from AR Powder. Extruded at 370° C. X 1400

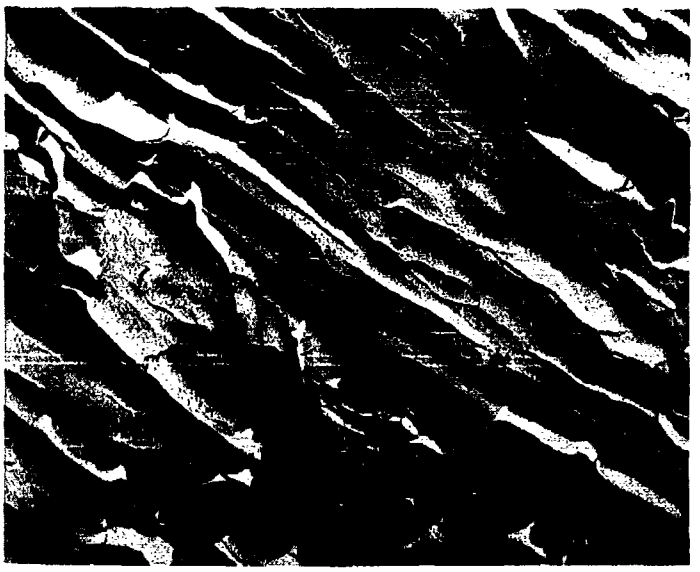

Figure 14(b) - Electron Micrograph of Fracture Surface on the Same Extrusion as shown in Fig. 13(b). X 5100

2. Extruded Monocrystals

Many of the observations made on the extruded powder material were repeated on the extruded monocrystals. Fully recrystallized specimens (extruded at 370°C), for example, both notched and unnotched, fractured by simple cleavage similar to Figures 12(a) and 13(a) with the exception that the grain size was larger and specular reflections from the individual cleavage facets were more easily recognized. Single crystals extruded at low temperatures and only partially recrystallized fractured over a locus which made an angle with the tensile axis. However, the fracture did not follow such an extreme path as that shown in Figure 12(c) but a zig-zag path similar to Figure 12(b) to leave the ragged surface shown in Figure 15. In the case of unnotched specimens, fracture started at the surface and followed a similar zig-zag path.

On cursory examination, the macrocopic appearance of these cold worked specimens led one to the conclusion that fracture had occurred by simple cleavage. Figure 16 shows for example the specular reflections observed on the surface of the specimen used for Figure 15. Optical examination at a higher magnification was somewhat complicated by the duplex nature of the microstructure indicated in Figures 2, 3, and 5 but it showed that while the recrystallized grains had definitely fractured by cleavage the cold worked fine grained regions had not. Their appearance was more typical of the fibrous fracture observed on silver chloride-alumina composites[2].

The true nature of the fracture mode in the heavily cold worked material was again revealed only when these regions were examined with the high resolution electron fractographic technique. The fracture surface then showed a very fine network of grain and sub grain boundaries as illustrated in Figure 17. This particular specimen was prepared from a single crystal extruded at -150°C and impacted at liquid nitrogen temperature. Although the surface was macroscopically very flat (thus accounting for the cleavage-like specular reflections of Figure 16) there were no cleavage lines and it was concluded that the fracture surface was again intergranular, except that the sub-grains were much smaller than those revealed in Figure 14(b) and were not so elongated.

2. Extruded Monocrystals

Many of the observations made on the extruded powder material were repeated on the extruded monocrystals. Fully recrystallized specimens (extruded at 370°C), for example, both notched and unnotched, fractured by simple cleavage similar to Figures 12(a) and 13(a) with the exception that the grain size was larger and specular reflections from the individual cleavage facets were more easily recognized. Single crystals extruded at low temperatures and only partially recrystallized fractured over a locus which made an angle with the tensile axis. However, the fracture did not follow such an extreme path as that shown in Figure 12(c) but a zig-zag path similar to Figure 12(b) to leave the ragged surface shown in Figure 15. In the case of unnotched specimens, fracture started at the surface and followed a similar zig-zag path.

On cursory examination, the macrocopic appearance of these cold worked specimens led one to the conclusion that fracture had occurred by simple cleavage. Figure 16 shows for example the specular reflections observed on the surface of the specimen used for Figure 15. Optical examination at a higher magnification was somewhat complicated by the duplex nature of the microstructure indicated in Figures 2, 3, and 5 but it showed that while the recrystallized grains had definitely fractured by cleavage the cold worked fine grained regions had not. Their appearance was more typical of the fibrous fracture observed on silver chloride-alumina composites[2].

The true nature of the fracture mode in the heavily cold worked material was again revealed only when these regions were examined with the high resolution electron fractographic technique. The fracture surface then showed a very fine network of grain and sub grain boundaries as illustrated in Figure 17. This particular specimen was prepared from a single crystal extruded at -150°C and impacted at liquid nitrogen temperature. Although the surface was macroscopically very flat (thus accounting for the cleavage-like specular reflections of Figure 16) there were no cleavage lines and it was concluded that the fracture surface was again intergranular, except that the sub-grains were much smaller than those revealed in Figure 14(b) and were not so elongated.

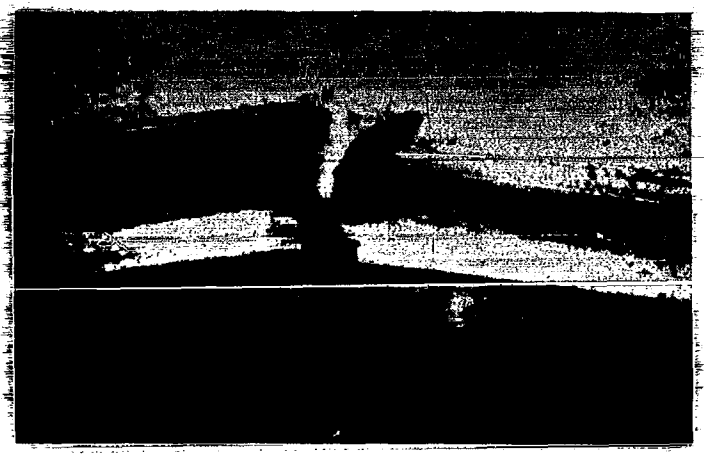

Figure 15 - Macroscopic View of Fracture Path of an Extrusion Made from Monocrystal Extruded at -25° C. X 6

Figure 16 - Macroscopic View of Fracture Surface on Specimen Shown in Fig. 15. X 8

Figure 17 - Electron Micrograph of Fracture Surface of an Extrusion Made from Monocrystal. Extruded at -150° C. X 2600

On the basis of these observations it was deduced that the low temperature extrusion of monocrystals produced a microstructure which consisted of a few recrystallized grains embedded in a severely distorted fine grained matrix.

To summarize the results of the fracture surface investigations:

(i) Both notched and unnotched specimens fracture in the same manner.

(ii) High temperature extrusion produces a fully recrystallized matrix which fractures by cleavage from an intergranular source.

(iii) Low temperature extrusion produces a highly distorted fine grained matrix which fractures intergranularly.

(iv) The respective modes are observed regardless of the source of material although the macroscopic appearance can be very different. Table 1 summarizes the fracture modes observed.

TABLE 1

MODE OF FRACTURE PROPAGATION SUMMARY

Extrusion Temperature	Extrusions from Monocrystals	Extrusions from Powder
370°C ($0.85\ T_m$)	Cleavage Figure 14(a)	Cleavage Figure 14(a)
Below 100°C ($0.5\ T_m$)	Intergranular Figure 17	Intergranular Figure 14(b)

V. DISCUSSION

The important observations of the preceding sections are the increased toughness of cold worked silver chloride at low temperatures and the change in fracture mode from clevage for fully recrystallized material to an intergranular mode for cold worked material. These observations must be interpreted in terms of the microstructure of the respective materials.

First we consider the behavior of extruded silver chloride powder specimens. From Figure 14(a) it is observed that in fully recrystallized silver chloride fracture prefers to proceed by clevage across the grains indicating this to be the path normally offering least resistance to crack propagation. On the other hand, in the cold worked material of Figure 14(b) it is noted that crack propagation now prefers to follow intergranular surfaces. Thus, cold work increases the resistance of the individual grains to clevage crack propagation. The exact mechanism that brings this about is not clear at the moment, but interaction of the crack front with the dislocation tangles and blunting of the crack tip by local slip from the high density of mobile dislocation sources could each contribute extra plastic work and cause the crack to stall.

The fact that fracture is forced to switch from clevage to intergranular propagation would not generally be expected to result in any great increase in toughness, but in the present case the microstructure and texture play an important role and must also be taken into consideration. The grains are elongated parallel with the extrusion direction and, therefore, parallel with the length of the impact specimen. To break such a specimen in two the fracture path cannot cut across the grains normally because of cold work, but is deflected to follow the intergranular surfaces and make a small angle with the tensile axis. This effectively blunts the crack and the specimen splinters into two as shown in Figure 12(c). In addition, because the specimens are so severly cold worked the intergranular surfaces themselves are not smooth but are distorted and roughened by the emerging slip steps. Thus, even intergranular propagation is affected by

cold work. It is believed that the lowering of the ductile brittle transition of the silver chloride powder extrusions in Figures 9 and 11 is due to the combination of these two factors; first an increase in the resistance to clevage crack propagation by cold work, and second, the fiber texture of the extruded material forcing intergranular propagation to occur over roughened surfaces parallel to the tensile axis.

It is considered that the behavior of extruded silver chloride single crystal specimens is besically the same. Due to cold work the fracture is again forced to follow an intergranular mode, but the grains in this material are not so elongated following extrusion and the fracture can follow a path more nearly normal to the tensile axis as shown in Figure 15. In addition, comparing Figures 14(b) and 17 it is apparent that the grain or subgrain size of the extruded monocrystal (1. 5μ by 4μ) is somewhat smaller than for the extruded powder (2μ by 10μ). Consequently the marked "geometrical" effect of grain shape on crack propagation through the extruded powder material is lost for the more equiaxed extruded single crystal material. It is suggested that this difference in texture explains why low temperature extrusion produces a much greater drop in the ductile brittle transition temperature for notched powder material (Figure 11) than for notched material of single crystal origin (Figure 10).

In terms of this interpretation there is now the question as to how much the resistance of a material to fracture can be modified by cold work. To learn more on this point the ductile brittle transition characteristics have been correlated with the compressive yield strength. Table II lists the compressive yield stress of various extrusions.

TABLE II

Comparison of Yield Stress (σ_y) with Extrusion Temperature

A. Extrusions Prepared with Monocrystals

Ext. Temp. ° C	σ_y, psi
370	1, 750
-72	4, 000
R. T.	4, 400
-25	4, 800
50	5, 250
-150	6, 150
-196	6, 400

B. Extrusions Prepared from AR Powder

Ext. Temp. ° C	σ_y, psi
370	3, 000
75	3, 950
50	4, 150
R. T.	4, 900
0	5, 280
-25	5, 650

The apparent anomaly in Table IIA wherein extrusions prepared from monocrystals at -72° C are less strong than those extruded at 50° C may be resolved in terms of the microstructure. For some reason, the material extruded at -72° C had recrystallized to a greater extent than the specimen extruded at 50° C presumable because the greater amount of stored cold work following low temperature working was relaxed by recrystallization at room temperature.

Otherwise, decreasing the extrusion temperature resulted in a more intensely cold worked matrix and a higher yield strength for both single crystal and powder material. It is interesting to note that the very low temperature single crystal extrusions (-150° C to -196° C) were significantly stronger than any of the extruded powder specimens.

Plotting these yield stress values against the mil-ductility temperatures for the corresponding extrusions, Figure 18 and 19 are obtained. It is important to point out that the extrusions prepared at 370° C were completely recrystallized and because of the great difference in microstructure should not be compared directly with the other extrusions, they were included on the figures merely to indicate the relative magnitude of the changes. Due to the semiquantitative nature of using yield stress to measure cold work and the difficulty in determining the nil-ductility temperature accurately a scatter in the results is to be expected.

From Figure 18 it is apparent that variations in the amount of cold work introduced by extruding single crystals at low temperatures have little or no effect on the ductile brittle transition. Thus, once the specimens are sufficiently worked to lower the nil-ductility temperature to -20° C the introduction of more cold work has no significant effect. On the other hand, for extrusions prepared from powder in Figure 19 there is a definite trend to indicate that the initial tendency for cold work to lower the nil-ductility temperature becomes reversed and that for excessive amounts of cold work the material is reembrittled. This is particularly noticeable for the powder extruded at -25° C which has a compressive strength of 5,650 psi but a nil-ductility temperature which has climbed from -180° C back up to -60° C. The reason for this change in behavior must again be associated with microstructure and is believed to be due to the fact that when precompressed powder is extruded at very low temperatures the cold welding of the individual particles does not result in good intergranular bonding and it is then easier for the intergranular cracks to propagate.

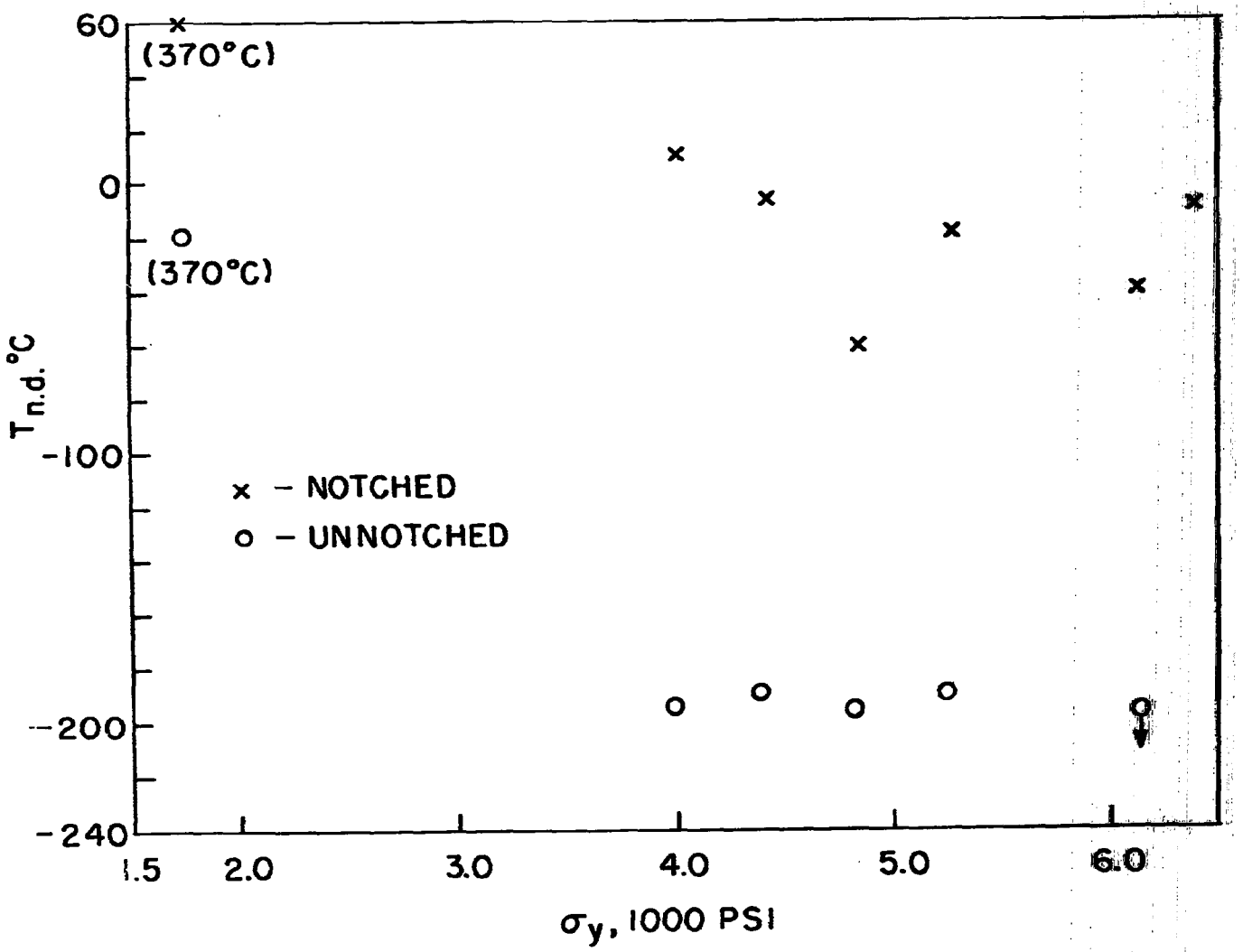

Figure 18 - Nil-ductility Temperatures vs. Yield Strength for Extrusions from Monocrystals

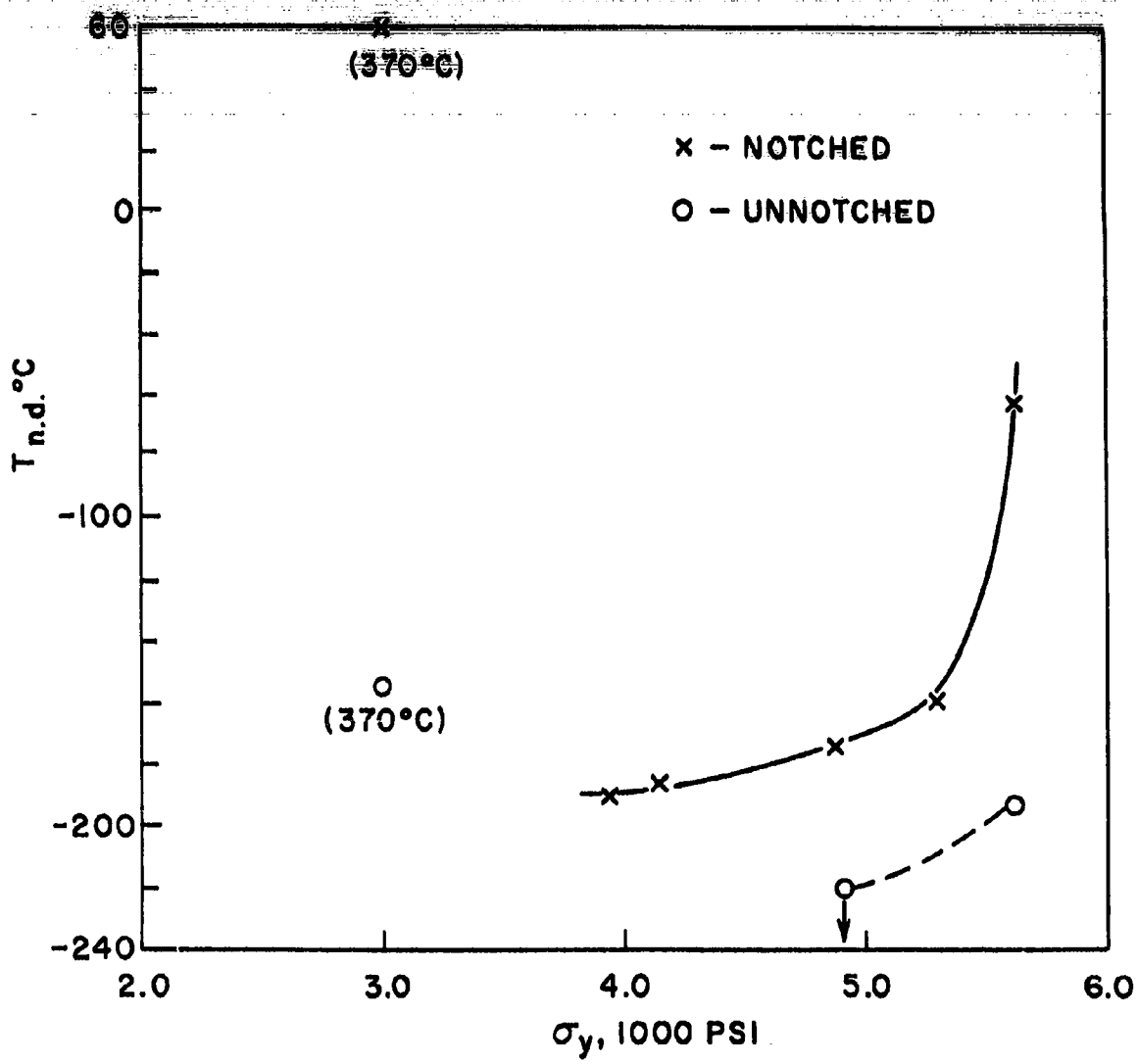

Figure 19 - Nil-ductility Temperature vs. Yield Strength for Extrusions from AR Powder.

In attempting to isolate the influence of cold work in this manner one may well question whether adequate consideration has been given to the influence of other variables such as grain size and texture. As mentioned previously, for the range of low extrusion temperatures used in this investigation, it is observed that the degree of preferred orientation remains unchanged and this is not believed to be an important factor. The influence of grain size cannot be so easile dismissed since the inherent inhomogeniety of cold work across the cross sections lends to local recrystallization in certain areas and severely distorted grains in others. By conventional methods it is difficult to arrive at a meaningful grain size for the various extrusions. However, close examination of fractured surfaces in the electron microscope has revealed that all extrusions from monocrystals (with the exception of those which recrystallized) had about the same grain size (1.5μ by 4μ) as did those extrusions from powder (2μ by 10μ). Thus, comparing results from a given source material as in Figures 18 and 19 is a fairly legitimate means for measuring the effect of cold work. Comparing results on material from different sources is confounded by the extra parameters of grain size and grain shape as has already been discussed.

To summarize, it is concluded that cold work by extrusion increases the resistance of individual silver chloride grains to clevage. Fracture is forced to propagate intergranularly over surfaces making a small angle with the tensile axis with a corresponding improvement in notch toughness. The angle of the fracture path is much smaller for extruded powder than for extruded single crystals because of the elongated grain shape. Increasing the amount of cold work by decreasing the extrusion temperature eventually causes reembrittlement of the powder due to a loss of intergranular cohesion.

At this point it is worthnoting that the modification of fracture mode and increase in toughness accomplished by the dispersion of spherical particles[2] may also result in part from change in the stored cold work and texture of the extruded material even though the extrusion temperature (370° C) is now well in the full recrystallization range.

There are other examples in the literature of the enhancement of notch toughness through the presence of longitudinal planes of weakness. In particular it has been shown by McEvily and Bush[4] that in the case of an ausformed steel, fracture prefers to follow the prior austenitic grain boundaries which due to the hot working are elongated parallel to the specimen axis. The appearance of their V-notch Charpy fractures are strikingly similar to those reproduced in Figure 12(c) of the present paper.

These observations should also be compared with the dependence of the bend ductility transition for tungsten containing low volume percent of oxides on the annealing treatment[5]. According to this work, as-rolled tungsten sheet shows a bend transition temperature at 140° C. This temperature is reduced to 80° C by a stress relief anneal at temperatures up to 1300° C, but beyond 1300° C where initial recrystallization or advanced recovery sets in, the bend ductility transition temperature is increased markedly. The drop of the nil-ductility temperature in silver chloride (Figure 19) from -60° C for severely cold work material and the marked increase up to 60° C for fully recrystallized material is quite similar to the above quoted tungsten results. We are currently examining the fracture surface appearance of tungsten broken under different conditions.

VI. CONCLUSIONS

Based on the results obtained and the foregoing discussion, the following conclusions are drawn:

(1) Cold working of silver chloride in the form of extrusion at temperatures where complete recrystallization does not take place decreases its impact nil-ductility temperature.

(2) After the initial decrease of nil-ductility temperature with cold working, additional stored cold work does not significantly affect the nil-ductility temperature for extrusions prepared from monocrystals.

(3) For silver chloride extrusions prepared from powder, initial cold working decreases the nil-ductility temperature, but additional stored cold work raises the nil-ductility temperature.

(4) Cold working by extrusion changes the fracture mode from clevage to an intergranular mode.

(5) It is condluded that cold work increases the resistance to crack propagation by clevage. The fracture is forced to occur intergranularly. The microstructure of extruded material causes fracture to follow an intergranular path almost parallel to the tension direction. These two factors combine to increase the toughness of silver chloride.

ACKNOWLEDGEMENTS

The authors are indebted to P. A. Talcott and D. J. Landis for much of the experimental work and to K. H. Olsen and S. Marquardt for providing the electron fractographs.

REFERENCES

1. T. L. Johnston, R. J. Stokes, and C. H. Li, Phil. Mag. 4, 1316 (1959). Fifth Technical Report to O. N. R.

2. T. L. Johnston, R. J. Stokes, and C. H. Li, Trans. AIME 221, 792 (1961). Eleventh Technical Report to O. N. R.

3. J. Friedel, Fracture, John Wiley and Sons, Inc. (New York), P. 498 (1959).

4. A. J. McEvily and R. H. Bush, Trans. A. S. M. 55, 654 (1962).

5. J. L. Ratcliff, D. J. Maykuth, H. R. Ogden, and R. I. Jaffee, "Development of a Ductile Tungsten Sheet Alloy", U. S. Navy BuWeps Summary Report Now 61-0677-C, May 1962.

TECHNICAL REPORT

Distribution List

Nonr-2456(00) NR032-451

Organization	No. of Copies
Chief of Naval Research Department of the Navy Washington 25, D.C. Attention: Code 423	(2)
Commanding Officer Office of Naval Research Branch Office 346 Broadway New York 13, New York	(1)
Commanding Officer Office of Naval Research Branch Office 495 Summer Street Boston 10, Massachusetts	(1)
Commanding Officer Office of Naval Research Branch Office 86 E. Randolph Street Chicago 1, Illinois	(1)
Commanding Officer Office of Naval Research Branch Office 1030 E. Green Street Pasadena 1, California	(1)
Commanding Officer Office of Naval Research Branch Office 1000 Geary Street San Francisco 9, California	(1)
Assistant Naval Attache for Research Office of Naval Research Branch Office, London Navy 100, Box 39 F.P.O., N.Y., N.Y.	(10)

Organization	No. of Copies
Director U.S. Naval Research Laboratory Washington 25, D.C. Attention: Technical Information Officer, Code 2000	(6)
: Code 2020	(1)
: Code 6200	(1)
: Code 6300	(3)
: Code 6100	(1)
Chief, Bureau of Naval Weapons Department of the Navy Washington 25, D.C. Attention: Code RRMA	(1)
: Code RREN-6	(1)
Commanding Officer U.S. Naval Air Material Center Philadelphia, Pennsylvania Attention: Aeronautical Materials Laboratory	(1)
Picatinny Arsenal Box 31 Dover, N.J. Attention: Lt. Hecht	(1)
Commanding Officer U.S. Naval Ordnance Laboratory White Oaks, Maryland	(1)
Commanding Officer U.S. Naval Proving Ground Dahlgren, Virginia Attention: Laboratory Division	(1)
Chief, Bureau of Ships Department of the Navy Washington 25, D.C. Attention: Code 315	(1)
335	(1)
341	(1)
350	(1)
364	(1)

Distribution List (Cont.)

Organization	No. of Copies
Commanding Officer U. S. Naval Engineering Experiment Station Annapolis, Maryland Attention: Metals Laboratory	(1)
Materials Laboratory New York Naval Shipyard Brooklyn 1, New York Attention: Code 907	(1)
Chief, Bureau of Yards and Docks Department of the Navy Washington 25, D. C. Attention: Research and Standards Division	(1)
Commanding Officer David Taylor Model Basin Washington 7, D. C.	(1)
Post Graduate School U. S. Naval Academy Monterey, California Attention: Dept. of Metallurgy	(1)
Office of Technical Services Department of Commerce Washington 25, D. C.	(1)
Commanding Officer U. S. Naval Ordnance Test Station Inyokern, California	(1)
Armed Services Technical Information Agency (ASTIA) Documents Service Center Arlington Hall Station Arlington, Va.	(5)
Commanding Officer Watertown Arsenal Watertown, Massachusetts Attention: Ordnance Materials Research Office	(1)
: Laboratory Division	(1)

Organization	No. of Copies
Commanding Officer Officer of Ordnance Research Box CM, Duke Station Duke University Durham, North Carolina Attention: Metallurgy Division	(1)
Commander Aeronautical Systems Division Wright-Patterson Air Force Base Dayton, Ohio Attention: Aeronautical Research	
: Lab. (WCRRL)	(1)
: Materials Laboratory (WCRTL)	(1)
: (ASRCEM-1)	(1)
U. S. Air Force ARDC Office of Scientific Research Washington 25, D. C. Attention: Solid State Division (SRQB)	(1)
National Bureau of Standards Washington 25, D. C. Attention: Metallurgy Division	(1)
: Mineral Products Division	(1)
National Aeronautics Space Administration Lewis Flight Propulsion Laboratory Cleveland, Ohio Attention: Materials and Thermodynamics Division	(1)
U. S. Atomic Energy Commission Washington 25, D. C. Attention: Technical Library	(1)
U. S. Atomic Energy Commission Washington 25, D. C. Attention: Metals and Materials Branch	(1)
Division of Research : Eng. Develop. Branch, Division of Reactor Development	(1)

Organization	No. of Copies
Argonne National Laboratory Library Services Dept. Report Section, Bldg 14-Room 14 9700 S. Cass Ave., Argonne, Ill.	(1)
Brookhaven National Laboratory Technical Information Division Upton, Long Island New York Attention: Research Library	(1)
Union Carbide Nuclear Co. Oak Ridge National Laboratory P. O. Box P Oak Ridge, Tennessee Attention: Metallurgy Division	(1)
: Solid State Physics Division	(1)
: Laboratory Records Dept.	(1)
Los Alamos Scientific Laboratory P. O. Box 1663 Los Alamos, New Mexico Attention: Report Librarian	(1)
General Electric Company P. O. Box 100 Richland, Washington Attention: Technical Information Division	(1)
Iowa State College P. O. Box 14A, Station A Ames, Iowa Attention: F. H. Spedding	(1)
Knolls Atomic Power Laboratory P. O. Box 1072 Schenectady, New York Attention: Document Librarian	(1)
U. S. Atomic Energy Commission New York Operations Office 70 Columbus Avenue New York 23, New York Attention: Document Custodian	(1)
Sandia Corporation Sandia Base Albuquerque, New Mexico Attention: Library	(1)
U. S. Atomic Energy Commission Technical Information Service Extension P. O. Box 62 Oak Ridge, Tennessee Attention: Reference Branch	(1)
University of California Radiation Laboratory Information Division Room 128, Building 50 Berkeley, California Attention: R. K. Wakerling	(1)
Bettis Plant U. S. Atomic Energy Commission Bettis Field P. O. Box 1468 Pittsburgh 30, Pennsylvania Attention: Mrs. Virginia Sternberg, Librarian	(1)
Commanding Officer and Director U. S. Naval Civil Engineering Laboratory Port Hueneme, California	(1)
Commanding Officer U. S. Naval Ordnance Underwater Station Newport, Rhode Island	(1)
U. S. Bureau of Mines Washington 25, D. C. Attention: Dr. E. T. Hayes	(1)
Defense Metals Information Center Battelle Memorial Institute 505 King Avenue Columbus, Ohio	(2)
Solid State Devices Branch Evans Signal Laboratory U. S. Army Signal Engineering Laboratories c/o Senior Navy Liaison Officer U. S. Navy Electronic Office Fort Monmouth, New Jersey	(1)

Organization	No. of Copies
U. S. Bureau of Mines P. O. Drawer B Boulder City, Nevada Attention: Electro-Metallurgical Div.	(1)
Commanding General U. S. Army Ordnance Arsenal, Frankford Philadelphia 37, Pennsylvania Attention: Mr. Harold Markus ORDBA-1320, 64-4	(1)
Prof. E. R. Parker Division of Mineral Technology University of California Berkeley 4, California	(1)
D. T. Bedsole, Manager, Technical Library Aerojet-General Corporation Sacramento, California	(1)
Dr. R. A. Lad National Advisory Committee for Aeronautics Lewis Flight Propulsion Laboratory Cleveland, Ohio	(1)
Prof. E. S. Machlin School of Mines Columbia University New York, New York	(1)
Dr. G. T. Murray Materials Research Corp. 47 Buena Vista Avenue Yonkers, New York	(1)
Prof. R. Smoluchowski School of Engineering Princeton University Princeton, New Jersey	(1)
Prof. P. Gibbs Department of Physics University of Utah Salt Lake City, Utah	(1)
Prof. F. H. Norton Department of Metallurgy Massachusetts Institute of Technology Cambridge 39, Massachusetts	(1)
Prof. J. J. Gilman Division of Engineering Brown University Providence, Rhode Island	(1)
Dr. R. G. Breckenridge National Carbon Research Laboratories P. O. Box 6116 Cleveland 1, Ohio	(1)
Dr. J. R. Low General Electric Research Laboratories P. O. Box 1088 Schenectady, New York	(1)
Prof. B. L. Averbach Department of Metallurgy Massachusetts Institute of Technology Cambridge 39, Massachusetts	(1)
Dr. O. L. Anderson Bell Telephone Laboratories Murray Hills, New Jersey	(1)
Prof. W. D. Kingery Department of Metallurgy Massachusetts Institute of Technology Cambridge 39, Massachusetts	(1)
Prof. D. S. Wood Department of Mechanical Engineering California Institute of Technology Pasadena, California	(1)

Organization	No. of Copies
Prof. T. S. Shevlin 303 Roberts Hall University of Washington Seattle 5, Washington	(1)
Dr. B. Post Polytechnic Institute of Brooklyn 99 Livingston Street Brooklyn, New York	(1)
Prof. G. C. Kuczynski University of Notre Dame Notre Dame, Indiana	(1)
Prof. W. H. Robinson Physics Department Carnegie Institute of Technology Pittsburgh, Pennsylvania	(1)
Prof. R. Roy Department of Geophysics Pennsylvania State University University Park, Pennsylvania	(1)
Dr. F. A. Halden Department of Chemistry Stanford Research Institute Menlo Park, California	(1)
Prof. D. H. Whitmore Department of Metallurgy Northwestern University Evanston, Illinois	(1)
Prof. P. J. Bray Department of Physics Brown University Providence, Rhode Island	(1)
Prof. J. O. Brittain Northwestern University Evanston, Illinois	(1)
Prof. W. R. Buessem Department of Ceramic Technology Pennsylvania State University University Park, Pennsylvania	(1)
Prof. A. L. Friedberg Department of Ceramic Engineering University of Illinois Urbana, Illinois	(1)
Prof. P. L. Edwards Texas Christian University Fort Worth, Texas	(1)
Prof. I. B. Cutler University of Utah Salt Lake City, Utah	(1)
Dr. B. Phillips Tem-Pres Research, Inc. State College, Pennsylvania	(1)
Prof. J. B. Wagner, Jr. Northwestern University Department of Materials Science Evanston, Illinois	(1)
Prof. W. C. Hahn Department of Metallurgy Montana School of Mines Butte, Montana	(1)
Prof. S. R. Butler Physics Department University of New Hampshire Durham, New Hampshire	(1)
Prof. F. Seitz Department of Physics University of Illinois Urbana, Illinois	(1)
Prof. H. Brooks Dean of Graduate School of Applied Science Harvard University Cambridge, Massachusetts	(1)
Dr. LeRoy R. Furlong Bureau of Mines College Park, Maryland	(1)

Organization	No. of Copies
Prof. W. G. Lawrence New York State College of Ceramics Alfred University Alfred, New York	(1)
Prof. A. von Hippel Laboratory for Insulation Research Massachusetts Institute of Technology Cambridge 39, Massachusetts	(1)
H. R. Peiffer RIAS Inc. 7212 Bellona Avenue Baltimore 12, Maryland	(1)
Prof. J. Gurland Division of Engineering Brown University Providence, Rhode Island	(1)
Dr. J. T. Ransom Engineering Research Laboratory Experiment Station E. I. duPont and Co., Inc. Wilmington, Delaware	(1)
Dr. F. J. P. Clarke Metallurgy Division A. E. R. E. Harwell, Berkshire, England	(1)
Dr. R. Chang Atomics International P. O. Box 309 Canoga Park, California	(1)
Dr. I. Cadoff New York University University Heights New York, New York	(1)
Prof. F. V. Lenel Department of Metallurgical Engineering Rensselaer Polytechnic Institute Troy, New York	(1)
Prof. J. A. Pask Dept. of Mineral Technology University of California Berkeley 4, California	(1)
Prof. D. Turnbull Div. of Engineering and Applied Physics Pierce Hall Harvard University Cambridge 38, Massachusetts	(1)
Dr. J. B. Wachtman, Jr. National Bureau of Standards Division 9.6 Washington 25, D. C.	(1)
Dr. J. J. Duga Battelle Memorial Institute 505 King Avenue Columbus 1, Ohio	(1)
Dr. W. P. Shulof Dept. 32-26 AC Spark Plug Division Flint, Michigan	(1)
Dr. R. M. Spriggs Metals and Ceramics Research AVCO Corp. 201 Lowell Street Wilmington, Massachusetts	(1)